https://doi.org/10.5194/tc-2023-154
Preprint. Discussion started: 10 October 2023

The Cryosphere Discussions
Open Access
EGU

A topographically-controlled tipping point for complete Greenland ice-sheet melt

Michele Petrini[1,2], Meike D.W. Scherrenberg[3], Laura Muntjewerf[4], Miren Vizcaino[5], Raymond Sellevold[6], Gunter R. Leguy[7], William H. Lipscomb[7], and Heiko Goelzer[1]

[1]NORCE Climate&Environment, Bjerknes Centre for Climate Research, Bergen, Norway
[2]National Institute of Oceanography and Applied Geophysics (OGS), Trieste, Italy
[3]Institute for Marine and Atmospheric research Utrecht (IMAU), Utrecht, Netherlands
[4]Royal Netherlands Meteorological Institute (KNMI), De Bilt, Netherlands
[5]Delft University of Technology (TUDelft), Delft, Netherlands
[6]Agder Energi, Kristiansand, Norway
[7]National Center for Atmospheric Research (NCAR), Boulder (CO), US

Correspondence: Michele Petrini (mpet@norceresearch.no)

Abstract.

A major impact of anthropogenic climate change is the triggering of tipping points, such as the complete mass loss of the Greenland ice sheet (GrIS). At present, the GrIS is losing mass at an accelerated rate, largely due to a steep decrease in its surface mass balance (SMB, the balance between snow accumulation and surface ablation from melt and associated runoff). Previous work on the magnitude and nature of a threshold for GrIS complete melt remains controversial. Here, we explore a potential SMB threshold for GrIS complete melt, and the processes controlling the nature of this threshold. To this end, we use the Community Ice Sheet Model v.2 (CISM2) forced with different levels of SMB previously calculated with the full-complexity Community Earth System Model v.2 (CESM2). The SMB calculation in CESM2 has been evaluated with contemporary observations and high-resolution modelling, and includes an advanced representation of surface melt and snow/firn processes.

We find a positive SMB threshold for complete GrIS melt of 230±84 Gt/yr, corresponding to a 60% decrease from the GrIS pre-industrial SMB. The ice-sheet response to sustained melt is highly non-linear, and determined by the effect of the SMB-height feedback in response to surface melt and Glacial Isostatic Adjustment (GIA). While the former process increases melt and promote runaway retreat, GIA-induced bedrock uplift stabilises the ice margin and delays deglaciation. The GrIS is tipping from ∼50% mass towards complete melt when the melt-induced surface lowering outweighs the GIA-induced bedrock uplift and the initially positive SMB becomes and remains negative for at least a few thousand years. We also find that the GrIS is tipping towards complete melt when the ice margin in the central west unpins from a coastal region with high bedrock elevation and SMB. Based on the minimum ice-sheet configuration in modelling studies of the GrIS during the last interglacial, we suggest that a stabilising effect of this midwestern topographic pinning point might have occurred in the past.

https://doi.org/10.5194/tc-2023-154
Preprint. Discussion started: 10 October 2023


The Cryosphere Discussions

1 Introduction

The Greenland Ice-Sheet (GrIS) is the largest freshwater reservoir in the northern Hemisphere, storing currently 7.42 m of Sea Level Equivalent (SLE, Morlighem et al., 2017). At present, the GrIS is losing mass at an accelerated pace, with ice loss rates over the last decade up to six times higher than in the 1980s (Mouginot et al., 2019). This is due to both atmospheric and ocean warming, causing enhanced surface melt and runoff, and increased ice discharge to the ocean (Mouginot et al., 2019). While until the late 1990s ice discharge has been the main source of ice loss, over the last two decades the contribution of surface processes has continuously increased, and as of today 50% of the overall GrIS mass loss increase is due to a decrease in Surface Mass Balance (SMB, *i.e.*, the balance between snow accumulation and surface ablation from melt and associated runoff) of around 160 Gt/yr (Mouginot et al., 2019; The IMBIE Team, 2020). In the future, the GrIS is expected to continue losing mass, with its contribution to Global Mean Sea-Level (GMSL) largely depending on the amount of greenhouse gas forcing to the climate system (0.01-0.10 m under SSP1-2.6, 0.09-0.18 m under SSP5-8.5 relative to 1995–2014, see Fox-Kemper, 2021, and references therein). Regardless of the emissions pathways, there is broad agreement that the GrIS mass loss over the 21st century and beyond will be dominated by SMB, while the influence of ice discharge to the ocean will diminish as the marine margins retreat to higher grounds (Robinson et al., 2012; Fürst et al., 2015; Goelzer et al., 2020; Gregory et al., 2020; Payne et al., 2021). Most of the projected decrease in SMB at the end of the century is attributed to an increase in surface melt and to the loss in refreezing capacity of the firn layer (Fettweis et al., 2013; Vizcaino et al., 2015; Sellevold and Vizcaíno, 2020; Noël et al., 2022). Over longer, multi-centennial and millennial timescales, another important source for future GrIS mass loss is the SMB-height feedback: *i.e.*, as the surface topography lowers due to ice thinning, the near surface air temperature warms and leads to further ice melt. A number of paleo and future ice-sheet modelling studies agree in showing that this self-amplifying mechanism can cause GrIS partial or near-complete melt over multi-millennia (Robinson et al., 2012; Levermann et al., 2013; Plach et al., 2019; Gregory et al., 2020), with ice loss possibly accelerated by the lower surface albedo in response to surface melt which tends to further decrease the SMB (SMB-albedo feedback: Box et al., 2012; Goelzer et al., 2016; Zeitz et al., 2021). Robinson et al. (2012) showed that while a negative integrated SMB is a sufficient condition for GrIS complete melt, not accounting for the evolving ice-sheet topography and SMB-height feedback (as done for example in Gregory and Huybrechts, 2006; Noël et al., 2021) is likely to result in an overestimation of the temperature threshold for ice-sheet loss. Modelling studies including this mechanism (either explicitly, or parametrized) estimated a Global Mean Temperature (GMT) threshold for GrIS complete melt over the next millennia between 1.6 K and 3 K above pre-industrial levels, with the rate of GrIS decline depending on the amount of warming above the threshold (Robinson et al., 2012; Levermann et al., 2013; Clark et al., 2016; Van Breedam et al., 2020; Gregory et al., 2020; Zeitz et al., 2022; Höning et al., 2023). Paleo data and modelling indicate that during the last interglacial period (LIG, ∼130-115 kyr BP) it is unlikely that the GMT exceeded 2 K above pre-industrial levels (Capron et al., 2014), and the GrIS contributed no more than 4 m to GMSL (Helsen et al., 2013; Goelzer et al., 2016; Plach et al., 2019; Sommers et al., 2021). This suggest that during the LIG the threshold for complete GrIS melt had not been passed, or the warming had been too little or too short to induce a full GrIS collapse. Another possible paleo-analogue for 21st century warming is the mid-Pliocene Warm Period (mPWP, ∼3.264-3.025 Myrs BP, Haywood et al., 2011), which is

https://doi.org/10.5194/tc-2023-154
Preprint. Discussion started: 10 October 2023

estimated to have been 2-3 K warmer than pre-industrial. GrIS simulations for this period yield extremely variable ice-sheet configurations, ranging from an ice-free state to a near modern GrIS depending on the climate forcing selected (Dolan et al., 2015). Altogether, paleo and future modelling studies both suggest the existence of a threshold for GrIS complete melt in a warmer climate; however, there is still uncertainty on the nature of this threshold, and whether or not the GrIS would exhibit a tipping point behaviour once this threshold is passed. A recent study using an ice-sheet model coupled to a low-resolution atmosphere Global Circulation Model (GCM) found a gradual, almost linear decline of GrIS equilibrium mass in response to sustained global mean warming (Gregory et al., 2020), rather than the sharp threshold behaviour found in earlier work (Robinson et al., 2012; Levermann et al., 2013). A better understanding of the mechanisms regulating the GrIS response to sustained warming is needed to determine the existence of tipping points for GrIS complete ice-sheet melt, and as such reduce uncertainties on the GrIS long-term Sea Level Rise (SLR).

Here, we determine a SMB threshold for GrIS complete melt, and we explore the processes controlling the nature of this threshold, as well as timing and pattern for GrIS decay. To this end, we use the higher-order Community Ice Sheet Model v.2 (CISM2, Lipscomb et al., 2019) forced with progressively decreasing SMB levels calculated with the full-complexity Community Earth System Model v.2 (CESM2, Danabasoglu et al., 2020) in a fully-coupled simulation of the global climate and GrIS (Muntjewerf et al., 2020b). The SMB calculation in CESM2 is based on a surface energy balance calculation, and includes an advanced representation of snow/firn processes, such as snow compaction, refreezing, and surface albedo (Muntjewerf et al., 2021; Sellevold and Vizcaíno, 2020). In our simulations, the SMB forcing is updated as the GrIS surface elevation evolves through an Elevation Classes (ECs) calculation in the land component of CESM2 (Muntjewerf et al., 2021), while bedrock changes due to Glacial Isostatic Adjustment (GIA) effect are accounted for in CISM2 through the Elastic Lithosphere-Relaxing Asthenosphere (ELRA) method (Lipscomb et al., 2019).

The paper is structured as follows: in Section 2, we briefly describe CISM2 (2.1), the SMB forcing (2.2) and the experimental setup (2.3). In Section 3 we analyse the main results, which are organised in three subsections on (3.1) thresholds, (3.2) pattern and timescales, and (3.3) processes for GrIS complete melt. In Section 4 we first discuss the thresholds found here in the context of the existing literature and end-of-century projections (4.1), and the existence of a tipping point for GrIS decay (4.2). We then draw our main conclusions and suggest possible future research directions (4.3).

2 Method

2.1 Ice-Sheet Model description

CISM2 is a parallel, three-dimensional thermomechanical ice-sheet Model (ISM) which solves equations for the conservation of mass, momentum, and internal energy (Lipscomb et al., 2019). In this study, CISM2 solves a depth-integrated viscosity approximation of the Stokes equations for incompressible viscous flow (DIVA, Goldberg, 2011). At the horizontal resolution used in this study for the Greenland domain (4 km), the DIVA outperformed other hybrid or zero-order solvers in terms of both model performance and representation of the ice-flow physics (Robinson et al., 2022). Basal sliding is calculated using a pseudo-plastic sliding law which incorporates linear, plastic and power-law behaviour (Aschwanden et al., 2016). Ocean

https://doi.org/10.5194/tc-2023-154
Preprint. Discussion started: 10 October 2023

forcing at the marine-terminating outlet glaciers is not accounted here, and floating ice is immediately removed based on a simple flotation criterion. GIA is parameterized using the Elastic-Lithosphere/Relaxing-Asthenosphere (ELRA) model (see for example Rutt et al., 2009), which allows to take account for a regional bedrock response to changes in ice load. The main CISM2 parameter values used in this study are provided in Table A1. Finally, while a more detailed description of all the CISM2 features and options can be found in Lipscomb et al. (2019), we highlight that the same model setup used here has been previously applied in fully coupled simulations of the global climate and the GrIS over the next centuries (Muntjewerf et al., 2020b, a) as well as in the past (Sommers et al., 2021).

2.2 SMB forcing

Here, we first provide a brief description of the general SMB calculation in CESM2 and how it is downscaled onto the CISM2 grid. Then, we describe the novel forcing method used in this study.

The SMB calculation is done in the land component of CESM2 (Community Land Model v.5, CLM5 Lawrence et al., 2019) and is defined as:

$$\begin{aligned} SMB =& Precipitation - Runoff - Sublimation; \\ Precipitation =& Rain + Snowfall; \\ Runoff =& Rain + Melt - Refreezing. \end{aligned}$$

Snowfall is calculated from the total precipitation depending on the surface temperature (100% snowfall if the temperature is below -2 K, 100% rain if the temperature is above 0 K, and linear interpolation in between). Rainfall can contribute positively to the SMB if it refreezes within the snowpack. Snow and ice melt are calculated based on the melt energy available within the ice column, which depends on the sum of net surface radiation, latent and sensible turbulent surface fluxes, and ground heat fluxes at the atmosphere-snow interface (Lawrence et al., 2019). In order to overcome the challenge of resolving steep SMB gradients around the ice-sheet margins at relatively coarse typical CLM5 resolutions (1°in Muntjewerf et al., 2020b), the SMB is calculated at 10 Elevation Classes (ECs), with boundaries at 0, 200, 400, 700, 1000, 1300, 1600, 2000, 2500, 3000, and 10000 m. This is done first by downscaling the CLM5 grid cell temperature to the EC elevation using a uniform lapse rate of -6 K/km. A vertically uniform relative humidity is then assumed to determine the potential temperature, specific humidity, air density, and surface pressure over each EC. The interpolated fields are then used to calculate the SMB components in each EC. After annual SMB is calculated at each EC in CLM5, it is then downscaled to the higher-resolution CISM2 domain through horizontal bilinear interpolation and linear vertical interpolation between adjacent ECs to the ice-sheet model surface elevation. More details on the SMB calculation and on the CESM2/CISM2 coupling are provided in Muntjewerf et al. (2021).

For this study, we use a functionality of CESM2 that allows to run CISM2 within the Earth System Model architecture, forced with multiple-ECs SMB previously calculated in CLM5. Under this setup, the SMB forcing fields are provided on the CLM5 grid. During runtime, every year the CESM2 coupler performs the trilinear (bilinear horizontal + linear vertical) interpolation to the surface elevation on the CISM2 4 km Greenland domain. In this way, the SMB is automatically updated

https://doi.org/10.5194/tc-2023-154
Preprint. Discussion started: 10 October 2023

during runtime for changes in ice-sheet geometry. This allows us to account for the SMB-height feedback based on snow/firn processes and energy fluxes at the ice-sheet surface.

2.3 Experimental setup

In this study, we force CISM2 with multiple-ECs SMB from a published, fully coupled CESM2/CISM2 simulation of the global climate and GrIS under an idealized, high Greenhouse Gas (GHGs) scenario (hereinafter referred to as BG-1pct run, Muntjewerf et al., 2020b). In this simulation, atmospheric CO_2 concentration is increased by 1% every year until it reaches four times pre-industrial values at year 140, after which it is kept fixed. From the BG-1pct run, we select several 23 years-long intervals corresponding to different SMB, and transient global mean and GrIS warming levels (values are shown in Table 1, see also Fig.1a). The choice of the intervals length results as a compromise between keeping the SMB standard deviation within the range of pre-industrial values and a sampling rate large enough to prevent data aliasing. In each simulation, we cycle the 23 years-long, multiple-ECs SMB forcing until a stable ice-sheet configuration is reached. Each run is restarted from the BG-1pct run at the last year of the corresponding forcing interval (initial and final year of each forcing interval are shown in Table A2). Additional sensitivity tests are performed by repeating some runs in which we (1) switch off the GIA parametrisation in CISM2 and (2) increase sliding velocities, by prescribing lower values (2.3°and 0.5°) of the minimum friction angle in the pseudo-plastic sliding law (see Table A1).

3 Results

Here we first describe the relationship between SMB forcing and final GrIS volume, to provide an SMB threshold for GrIS complete melt. We then illustrate the pattern and timescales for ice retreat, in particular for simulations close to the SMB threshold. We conclude by assessing the processes that determine the GrIS response to sustained warming.

3.1 Thresholds for GrIS complete melt

In our simulations, the GrIS exhibit a sharp threshold behaviour, with a highly non-linear relatioship between initial SMB forcing and final GrIS mass (Fig. 1b). In Table 1 the SMB forcing, the corresponding transient global mean and GrIS warming above pre-industrial, and the resulting final GrIS volume are provided for each run. Final GrIS states are clustered in three main groups: (a) “low melt”, with less than 25% GrIS mass loss (b) “medium melt”, with around 50% GrIS mass loss, (c) “complete melt”, with more than 80% GrIS mass loss. GrIS limited loss (<25%) is obtained for an initial SMB forcing above 317±97 Gt/yr, and transient global mean and GrIS warming above pre-industrial below 2.8 K and 2.2 K, respectively. Compared to the fully coupled CESM2/CISM2 pre-industrial control simulation (hereafter BG-PIcontrol run, Lofverstrom et al., 2020, see Table 2), this means that low GrIS melt is achieved for a decrease in SMB not exceeding 50% of the equilibrium pre-industrial SMB. An ice loss of around 50% of the initial GrIS mass is obtained for intermediate SMB forcing (between 40 and 50% of the pre-industrial equilibrium SMB) and global mean warming values (between 2.8 and 3.4 K above pre-industrial). We find that the GrIS is bound to completely melt if the initial SMB forcing is lower than 230±84 Gt/yr (Fig. 1b and Table 1). This is a

https://doi.org/10.5194/tc-2023-154
Preprint. Discussion started: 10 October 2023

150 decrease of around 60% of the GrIS equilibrium SMB at the end of the BG-PIcontrol run. The SMB threshold corresponds, in the BG-1pct run, to a transient global mean and GrIS warming above pre-industrial of 3.4 K and 3.2 K, respectively (Fig. 1a and Table 1).

3.2 Pattern and timescales of GrIS retreat

In the "low melt" simulations, ice loss mostly takes place at the southwestern margin, with limited retreat in the north occurring
155 in the +2.8 K run (see inset in Fig. 1b). The southwestern GrIS margin retreats all the way to the east in the "medium melt" simulations, until a large ice cap in the southern tip of Greenland is disconnected from the GrIS main body. In these simulations, showing an intermediate GrIS loss, significant retreat also occurs in the north, whereas the midwestern ice-sheet margin remains close to the coast (see inset in Fig. 1b). When the SMB threshold for complete GrIS melt is passed, the GrIS retreats all the way towards the east, with isolated ice caps of variable size remaining in regions of high bedrock elevation (see inset in Fig.
160 1b). Timescales for ice loss increase sharply as the initial SMB forcing gets close to the threshold for GrIS complete mass loss. In the "low melt" simulations, minimum GrIS volume is reached within the first 15 kyrs (Fig. 2 and Table 1). Timescales are doubled for the "medium melt" simulations, in which the GrIS attains minimum volume after around 30-35 kyrs. The simulation immediately above the SMB threshold (+3.4 K run) shows the highest response time, as the GrIS keeps decreasing until 40 kyrs, after a retreat slowdown between 15 and 20 kyrs (Fig. 2 and Table 1). For the other simulations in the "complete
165 melt" group, timescales decrease quickly as the initial SMB forcing gets lower and moves away from the threshold. For a positive initial SMB forcing, the shortest GrIS deglaciation time is around 12 kyrs, whereas if the initial SMB forcing is negative Greenland becomes mostly ice-free in 8 kyrs or less (Fig. 2). Detailed GrIS retreat pattern and timescales for each simulation are displayed in Supplementary Videos V1-10.

3.3 Processes controlling ice retreat

170 In our simulations, the response of the GrIS to sustained warming is primarily determined by the interplay of surface melt and GIA, which are interconnected through the SMB-height feedback. For every initial SMB forcing level, the ice-sheet loses mass during the first 10-15 kyrs, and the SMB further decreases due to ice thinning and surface elevation lowering (Fig. 2). However, the impact of ice thinning is mitigated, and in some cases counterbalanced, by GIA: while the ice sheet thins and retreat, the bedrock uplifts, thus increasing the surface elevation and, consequently the SMB (see bottom panel in Fig. 2 and Supplementary
175 Video xxx). This interplay is key in determining whether the ice-sheet will disappear or not: GrIS complete loss is achieved only in simulations where the surface lowering outweighs the bedrock uplift, and the SMB becomes and remains negative for at least a few thousand years (Fig.2). When this does not happen, the GrIS eventually reaches a more stable configuration as in the "low melt" or "medium melt" groups. In the simulations that are closest to the threshold for complete GrIS melt, the interplay of SMB-height feedback and GIA is also causing self-sustained, quasi-periodic ice-sheet oscillations ranging
180 between 3% and 12% of the initial GrIS mass. In fact, in some cases the increase in SMB due to GIA-induced bedrock uplift can promote ice thickening and margin readvance. This mechanism is then reverted when the isostatic subsidence resulting from ice thickening causes the SMB to decrease again, enough to promote ice thinning and margin retreat (see Supplementary

https://doi.org/10.5194/tc-2023-154
Preprint. Discussion started: 10 October 2023

Videos). The amplitude and periodicity of these oscillation increase as the initial SMB forcing gets closer to the threshold for complete GrIS melt. The highest oscillation amplitude and periodicity is obtained in the simulation immediately after the SMB threshold is crossed (+3.2 K run, with a volume oscillations of 12% of the initial ice mass and over cycles of 30 kyrs, see Fig. A1). If GIA is switched off, the response of the GrIS changes drastically. When we turn off GIA for a simulation in the "medium melt" group (+3.2 K run), SMB-height feedback due to surface lowering alone causes a rapid deglaciation in 10 kyrs (Fig.3). This is equivalent, both in terms of final GrIS mass and timing response, to a simulation in the "complete melt" group, with an initial SMB forcing well above the threshold (+4.0 K run). For other simulations in the "complete melt" group, removing the GIA effect greatly reduces the timescales for GrIS destabilization and substantial mass loss, except when the original timescales are already shorter than 5 kyrs with isostasy included (Fig.3). Our sensitivity tests (described in Subsection 2.3) also show that ice discharge does not play a role in determining the long-term GrIS equilibrium response to sustained warming. In fact, while the increase in ice discharge affects the overall GrIS mass budget over centuries, the long-term ice-sheet response remains unchanged, and is determined solely by the SMB evolution (see Fig. A2).

A comparison of the simulations immediately below and above the SMB threshold for GrIS complete melt (+3.2 K and +3.4 K runs, Fig. 4) indicates that the ice margin position in the central west is crucial to determine the final ice-sheet state. In particular, a group of isolated ice caps with high bedrock elevation and SMB (Fig. 4 and A3) act as a topographic pinning point for the GrIS. In fact when the ice margin remains sufficiently close to these topographic highs to reestablish connection during margin readvances within self-sustained oscillations, the ice loss in the southwest and north remains limited (see left panel in Fig. 4 and Supplementary Video V5). When instead the midwestern margin loses permanently contact with the topographic pinning point, the SMB-height feedback causes a runaway ice retreat towards the east, and more than 80% of the GrIS mass is lost. This tipping behaviour is clear in the first simulation above the SMB threshold (+3.4 K run, see central panel in Fig. 4), with the runaway retreat occurring only after 20 kyrs, when the connection between the ice sheet and the topographic pinning point is permanently lost. In the remaining simulations after the SMB threshold is crossed, the connection between the midwestern margin and the topographic pinning point is lost earlier (around 15 kyrs or less) and the retreat pattern is more uniform in time (see right panel in Fig. 4, A4 and Supplementary Videos V5-7).

4 Discussion

In this section, we compare the thresholds found here with the existing literature. Even though our simulations are not meant to represent realistic scenarios, we will also try to put the thresholds found here in the context of end-of-century future projections. Then, we will discuss the GrIS tipping point behaviour and the stabilizing effect of the topographic pinning point found in the central west. We will then summarise our conclusions and suggest possible future research directions.

4.1 Thresholds for complete GrIS melt

Here we have found a positive SMB threshold of 230±84 Gt/yr for complete GrIS melt. This corresponds to a 60% decrease from the GrIS equilibrium SMB calculated in the BG-PIcontrol run (591±83 Gt/yr, see Table 2 and Lofverstrom et al., 2020). In

https://doi.org/10.5194/tc-2023-154
Preprint. Discussion started: 10 October 2023

this pre-industrial run, no corrections are applied to the SMB, and the GrIS is left free to evolve. Although CESM2 compares reasonably well with ERA-Interim and RACMO2 for several key controls on GrIS SMB (surface melt, runoff, longwave radiation van Kampenhout et al., 2020; Noël et al., 2020), this approach led to an overestimation of the GrIS initial extent (15%), volume (13%) and as a consequence, of a pre-industrial SMB, which is higher than in uncoupled CESM2 experiments and present-day observations (see Table 2 and Lofverstrom et al., 2020). In view of this, the positive SMB threshold found here is coupled-model dependent, and it remains complicated to analyse in the context of end-of-century projections, or to make a direct comparison with other modelling studies and recent observations. Constraining ISM simulations to GrIS changes during the LIG, Robinson et al. (2012) found a positive SMB threshold for complete ice-sheet melt ranging between 150-340 Gt/yr. This agrees reasonably well with our study, although in Robinson et al. (2012) the pre-industrial SMB is lower (around 400 Gt/yr). In the fully coupled CESM2/CISM2 projection for the SSP5-8.5 scenario, the SMB crosses our threshold for GrIS instability between years 2060-2080, and by the end of the century it has become negative (Muntjewerf et al., 2020a). In our simulations, a negative SMB forcing leads to a relatively rapid GrIS deglaciation in less than 10 kyrs (Table 1 and Fig. 2). While fully coupled CESM2/CISM2 simulations for lower emission scenarios (SSP1-2.6, SSP2-4.5, SSP3-7.0) are currently not available, in the corresponding CESM2-only future projections the SMB over the GrIS at the end of the century is well below the threshold found here, regardless of the emission scenario considered (see Table 2). This comparison, however, must be considered carefully as (a) the GrIS pre-industrial SMB is lower in CESM2-only runs, (b) in CESM2-only runs, the SMB is calculated over a fixed present-day GrIS topography, and as such the SMB-height feedback is not accounted for.

The SMB threshold found here corresponds to a transient global mean and GrIS warming of 3.4 K and 3.2 K above pre-industrial, respectively. Our global mean warming threshold is at the high end of previous ice-sheet modelling studies with climate forcing (a) calculated offline with GCMs (3.1 K, Gregory and Huybrechts, 2006) (b) interactively calculated with regional models or intermediate complexity Earth System Models (1.6-3 K, Robinson et al., 2012; Levermann et al., 2013; Gregory and Huybrechts, 2006; Höning et al., 2023). We highlight however that in our forcing method the SMB has not fully equilibrated with the climate, and a more sustained warming of 3.4 K above pre-industrial would likely result in a lower SMB as the snow pack deteriorates (ablation area expansion, less refreezing capacity). To properly determine a global mean warming threshold for complete GrIS melt would require running further CESM2/CISM2 fully or asynchronously coupled experiments, which is computationally too expensive and out of the scope of this study.

4.2 GrIS tipping point behaviour

Our simulations indicate that the GrIS response to sustained warming is highly non-linear, and that the ice-sheet is tipping from 50% mass towards complete melt once that the positive SMB threshold is passed. This agrees well with early modelling studies (Gregory and Huybrechts, 2006; Robinson et al., 2012; Levermann et al., 2013). However, this is in contradiction with the results presented in Gregory et al. (2020), which suggests a gradual, almost linear GrIS decline in response to sustained global mean warming. In their study, Gregory et al. (2020) used an ISM coupled to a low-resolution atmosphere GCM, and adopted a similar EC approach as done in CESM2 for the SMB calculation. Here, CISM2 is not bi-directionally coupled to CESM2, and as such we do not account for increased cloudiness and snowfall as the ice-sheet margin moves towards the

https://doi.org/10.5194/tc-2023-154
Preprint. Discussion started: 10 October 2023

interior. In Gregory et al. (2020), these processes result in an increase in precipitation which in some cases counterbalances the SMB-height feedback and lead to the multiple stable GrIS states. However, in our simulations the GrIS tipping behaviour is determined by the interplay of SMB-height feedback and GIA, with the latter not being accounted for in Gregory et al. (2020). While we cannot exclude that accounting for ice-sheet/atmospheric circulation feedbacks would stabilise the GrIS and change the SMB threshold, it is also difficult to determine if they would drastically change the non-linear nature of the GrIS response to sustained warming found here. Another recent study by Zeitz et al. (2022) found a similar, non-linear impact of the interplay between GIA and SMB-height on the GrIS response to sustained warming, with final GrIS states clustered in three main groups for a global warming exceeding 2 K above pre-industrial ("partial recovery", "oscillations", "loss"). Zeitz et al. (2022) used a different ISM and GIA parametrisation than in our study, thus suggesting that the GrIS tipping behaviour simulated here is unlikely to depend on our model setup. Our study also agrees well with (Zeitz et al., 2022; Plach et al., 2019) in showing that increased ice discharge rates have no effect on the long-term GrIS equilibrium response to sustained warming.

We find that the GrIS is tipping towards complete melt if the ice margin in the central west retreats enough to disconnect from a group of isolated ice caps with high bedrock elevation and SMB. If the ice margin remains pinned to this topographic pinning point, GrIS loss is limited also in southwestern and northern Greenland, and does not exceed 50% of the initial GrIS mass. The presence of this topographic feature of the GrIS, in combination with a stable midwestern margin position and limited ice loss in the southwest and north has been consistently simulated in ice-sheet modelling studies of the LIG (Helsen et al., 2013; Plach et al., 2019; Goelzer et al., 2016; Sommers et al., 2021). In these simulations, the midwestern margin remains pinned to the topographic pinning point, and the GrIS does not lose more than 4 m SLE. In particular, in the fully coupled CESM2/CISM2 simulation of the LIG, the GrIS extent at 123 kyrs ago is extremely similar to those in our simulations belonging to the 'medium melt' group (see Fig. 3 in Sommers et al., 2021). After this time, however, the SMB becomes positive and the GrIS starts to readvance towards the west. This suggests that around 123 kyrs the GrIS might have been close to tipping towards a much reduced state. Compared with other modelling studies indicating a GrIS tipping point behaviour in response to sustained warming, our study agrees in showing that the ice-sheet retreats towards the east, and that the midwestern margin remains close to the coast before tipping (Robinson et al., 2012; Höning et al., 2023; Zeitz et al., 2022).

4.3 Conclusions and future research

Here, we have used a state-of-the-art, higher-order Ice-Sheet Model (CISM2) to (1) determine a SMB threshold for GrIS complete melt, (2) investigate the nature of this threshold, (3) understand the processes controlling the ice-sheet response. We forced CISM2 with different levels of SMB, previously calculated at multiple Elevation Classes with a full-complexity Earth-System Model (CEMS2) which includes an advanced representation of snow/firn processes, surface albedo and melt. In our simulations, the SMB is updated as the ice-sheet surface elevation changes through the Elevation Classes (ECs) method, and bedrock changes due to GIA effects are accounted for in CISM2 through the ELRA parametrization.

We have found a positive SMB threshold for complete GrIS melt of 230±84 Gt/yr, corresponding to a 60% decrease from the GrIS pre-industrial equilibrium SMB. This SMB threshold corresponds to a transient global mean and GrIS warming of 3.4 K and 3.2 K above pre-industial, respectively. The thresholds found here are in overall agreement with previous studies. In our

https://doi.org/10.5194/tc-2023-154
Preprint. Discussion started: 10 October 2023

simulations, the response of GrIS to sustained warming is highly non-linear, and final ice-sheet state are clustered in three main groups: (a) "low melt" (<25% mass loss), (b) "medium melt" (∼50% mass loss), (c) "complete melt" (>80% mass loss). This tipping behaviour is determined by the effect of SMB-height feedback in response to surface melt and GIA. While topographic lowering due to surface melt promote further melt and ice loss, GIA causes a bedrock uplift which yields in turn reduced melt, ice thickening and margin stabilisation or readvance. The GrIS is tipping from ∼50% mass towards complete loss when the melt-induced surface lowering outweighs the GIA-induced bedrock uplift, and the initially positive SMB becomes and remains negative for at least a few thousand years. A similar tipping behaviour of the GrIS, resulting from the interplay of SMB-height feedback and GIA, has been also simulated in other studies. However, literature also suggests that ice-sheet/atmosphere stabilising feedbacks might dampen the non-linear response of the GrIS to sustained warming. We also found that whether the GrIS will tip towards complete melt or not depends on the ice-sheet margin position in the central west. When the ice margin remains pinned to a coastal region with high bedrock elevation and SMB, GrIS loss is limited also in the southwest and north and remains close to ∼50% of its initial mass. Previous modelling studies of the GrIS during the LIG show that the ice-sheet had, at its minimum extent, a similar configuration as in our simulations in the "medium melt" group. In view of this, we suggest that a stabilising effect of the midwestern topographic pinning point might also have occurred during the LIG.

The modelling approach presented here incldues an advanced representation of the SMB-height and albedo feedback through the CESM2 melt energy calculation, snow/firn model and Elevation Classes approach. Nevertheless, the main caveat of this study is that CISM2 is not bi-directionally coupled to CESM2, and as such we do not account for a number of ice-sheet/atmosphere feedbacks (*e.g.*, increase in cloud cover and precipitation as the GrIS retreats towards the interior). To better understand the nature of the response of the GrIS to sustained warming, further coupled modelling (and as such, computational) efforts should be dedicated to fully resolve how these negative feedbacks interact with SMB-height feedback and GIA. In addition, future modelling studies of the GrIS during the LIG could shed light on how close the GrIS might have been to tipping at its minimum extent, and which processes might have prevented that.

Code and data availability. CESM2 is an open source model, available at https://www.cesm.ucar.edu. Computing and data storage resources, including the Cheyenne supercomputer (doi:10.5065/D6RX99HX), were provided by the Computational and Information Systems Laboratory (CISL) at NCAR. Forcing files from the fully coupled simulations and setup scripts to reproduce our simulations are stored in the Cheyenne supercomputer and available upon request.

Video supplement. Supplementary Videos can be found on Zenodo (https://doi.org/10.5281/zenodo.8384527).

Author contributions. MV planned the research; MS performed an initial set of simulations; MP performed the remaining simulations, analysed the output and wrote the manuscript. All authors discussed the results and reviewed and edited the manuscript.

https://doi.org/10.5194/tc-2023-154
Preprint. Discussion started: 10 October 2023

Competing interests. The contact author has declared that none of the authors has any competing interests.

Acknowledgements. The CESM project is supported primarily by the National Science Foundation (NSF). This material is based upon work supported by the National Center for Atmospheric Research, which is a major facility sponsored by the NSF under Cooperative Agreement 1852977. MP, MV, LM, and RM have received funding from the European Research Council (Grant ERC-StG-678145-CoupledIceClim). MP and HG have received funding from the Research Council of Norway under projects 324639. Storage resources were also provided by the Norwegian infrastructure for computational science (through project NS8006K).

https://doi.org/10.5194/tc-2023-154
Preprint. Discussion started: 10 October 2023

References

Aschwanden, A., Fahnestock, M. A., and Truffer, M.: Complex Greenland outlet glacier flow captured, Nature communications, 7, 10 524, 2016.

Box, J., Fettweis, X., Stroeve, J., Tedesco, M., Hall, D., and Steffen, K.: Greenland ice sheet albedo feedback: thermodynamics and atmospheric drivers, The Cryosphere, 6, 821–839, 2012.

Capron, E., Govin, A., Stone, E. J., Masson-Delmotte, V., Mulitza, S., Otto-Bliesner, B., Rasmussen, T. L., Sime, L. C., Waelbroeck, C., and Wolff, E. W.: Temporal and spatial structure of multi-millennial temperature changes at high latitudes during the Last Interglacial, Quaternary Science Reviews, 103, 116–133, 2014.

Clark, P. U., Shakun, J. D., Marcott, S. A., Mix, A. C., Eby, M., Kulp, S., Levermann, A., Milne, G. A., Pfister, P. L., Santer, B. D., et al.: Consequences of twenty-first-century policy for multi-millennial climate and sea-level change, Nature climate change, 6, 360–369, 2016.

Danabasoglu, G., Lamarque, J.-F., Bacmeister, J., Bailey, D., DuVivier, A., Edwards, J., Emmons, L., Fasullo, J., Garcia, R., Gettelman, A., et al.: The community earth system model version 2 (CESM2), Journal of Advances in Modeling Earth Systems, 12, e2019MS001 916, 2020.

Dolan, A., Hunter, S., Hill, D., Haywood, A., Koenig, S., Otto-Bliesner, B. L., Abe-Ouchi, A., Bragg, F., Chan, W.-L., Chandler, M., et al.: Using results from the PlioMIP ensemble to investigate the Greenland Ice Sheet during the mid-Pliocene Warm Period, Climate of the Past, 11, 403–424, 2015.

Fettweis, X., Franco, B., Tedesco, M., Van Angelen, J., Lenaerts, J. T., van den Broeke, M. R., and Gallée, H.: Estimating the Greenland ice sheet surface mass balance contribution to future sea level rise using the regional atmospheric climate model MAR, The Cryosphere, 7, 469–489, 2013.

Fox-Kemper, B.: Ocean, cryosphere and sea level change, in: AGU Fall Meeting Abstracts, vol. 2021, pp. U13B–09, 2021.

Fürst, J. J., Goelzer, H., and Huybrechts, P.: Ice-dynamic projections of the Greenland ice sheet in response to atmospheric and oceanic warming, The Cryosphere, 9, 1039–1062, 2015.

Goelzer, H., Huybrechts, P., Loutre, M.-F., and Fichefet, T.: Last Interglacial climate and sea-level evolution from a coupled ice sheet–climate model, Climate of the Past, 12, 2195–2213, 2016.

Goelzer, H., Nowicki, S., Payne, A., Larour, E., Seroussi, H., Lipscomb, W. H., Gregory, J., Abe-Ouchi, A., Shepherd, A., Simon, E., et al.: The future sea-level contribution of the Greenland ice sheet: a multi-model ensemble study of ISMIP6, The Cryosphere, 14, 3071–3096, 2020.

Goldberg, D. N.: A variationally derived, depth-integrated approximation to a higher-order glaciological flow model, Journal of Glaciology, 57, 157–170, 2011.

Gregory, J. and Huybrechts, P.: Ice-sheet contributions to future sea-level change, Philosophical Transactions of the Royal Society A: Mathematical, Physical and Engineering Sciences, 364, 1709–1732, 2006.

Gregory, J. M., George, S. E., and Smith, R. S.: Large and irreversible future decline of the Greenland ice sheet, The Cryosphere, 14, 4299–4322, 2020.

Haywood, A., Dowsett, H. J., Robinson, M. M., Stoll, D. K., Dolan, A., Lunt, D., Otto-Bliesner, B., and Chandler, M.: Pliocene Model Intercomparison Project (PlioMIP): experimental design and boundary conditions (experiment 2), Geoscientific Model Development, 4, 571–577, 2011.

https://doi.org/10.5194/tc-2023-154
Preprint. Discussion started: 10 October 2023

Helsen, M., Van De Berg, W., Van De Wal, R., Van Den Broeke, M., and Oerlemans, J.: Coupled regional climate–ice-sheet simulation shows limited Greenland ice loss during the Eemian, Climate of the Past, 9, 1773–1788, 2013.

Höning, D., Willeit, M., Calov, R., Klemann, V., Bagge, M., and Ganopolski, A.: Multistability and transient response of the Greenland ice sheet to anthropogenic CO2 emissions, Geophysical Research Letters, 50, e2022GL101 827, 2023.

Lawrence, D. M., Fisher, R. A., Koven, C. D., Oleson, K. W., Swenson, S. C., Bonan, G., Collier, N., Ghimire, B., van Kampenhout, L., Kennedy, D., et al.: The Community Land Model version 5: Description of new features, benchmarking, and impact of forcing uncertainty, Journal of Advances in Modeling Earth Systems, 11, 4245–4287, 2019.

Levermann, A., Clark, P. U., Marzeion, B., Milne, G. A., Pollard, D., Radic, V., and Robinson, A.: The multimillennial sea-level commitment of global warming, Proceedings of the National Academy of Sciences, 110, 13 745–13 750, 2013.

Lipscomb, W. H., Price, S. F., Hoffman, M. J., Leguy, G. R., Bennett, A. R., Bradley, S. L., Evans, K. J., Fyke, J. G., Kennedy, J. H., Perego, M., et al.: Description and evaluation of the community ice sheet model (CISM) v2. 1, Geoscientific Model Development, 12, 387–424, 2019.

Lofverstrom, M., Fyke, J. G., Thayer-Calder, K., Muntjewerf, L., Vizcaino, M., Sacks, W. J., Lipscomb, W. H., Otto-Bliesner, B. L., and Bradley, S. L.: An efficient ice sheet/Earth system model spin-up procedure for CESM2-CISM2: Description, evaluation, and broader applicability, Journal of Advances in Modeling Earth Systems, 12, e2019MS001 984, 2020.

Morlighem, M., Williams, C. N., Rignot, E., An, L., Arndt, J. E., Bamber, J. L., Catania, G., Chauché, N., Dowdeswell, J. A., Dorschel, B., et al.: BedMachine v3: Complete bed topography and ocean bathymetry mapping of Greenland from multibeam echo sounding combined with mass conservation, Geophysical research letters, 44, 11–051, 2017.

Mouginot, J., Rignot, E., Bjørk, A. A., Van den Broeke, M., Millan, R., Morlighem, M., Noël, B., Scheuchl, B., and Wood, M.: Forty-six years of Greenland Ice Sheet mass balance from 1972 to 2018, Proceedings of the national academy of sciences, 116, 9239–9244, 2019.

Muntjewerf, L., Petrini, M., Vizcaino, M., Ernani da Silva, C., Sellevold, R., Scherrenberg, M. D., Thayer-Calder, K., Bradley, S. L., Lenaerts, J. T., Lipscomb, W. H., et al.: Greenland Ice Sheet contribution to 21st century sea level rise as simulated by the coupled CESM2. 1-CISM2. 1, Geophysical Research Letters, 47, e2019GL086 836, 2020a.

Muntjewerf, L., Sellevold, R., Vizcaino, M., Ernani da Silva, C., Petrini, M., Thayer-Calder, K., Scherrenberg, M. D., Bradley, S. L., Katsman, C. A., Fyke, J., et al.: Accelerated Greenland ice sheet mass loss under high greenhouse gas forcing as simulated by the coupled CESM2. 1-CISM2. 1, Journal of Advances in Modeling Earth Systems, 12, e2019MS002 031, 2020b.

Muntjewerf, L., Sacks, W. J., Lofverstrom, M., Fyke, J., Lipscomb, W. H., Ernani da Silva, C., Vizcaino, M., Thayer-Calder, K., Lenaerts, J. T., and Sellevold, R.: Description and Demonstration of the Coupled Community Earth System Model v2–Community Ice Sheet Model v2 (CESM2-CISM2), Journal of Advances in Modeling Earth Systems, 13, e2020MS002 356, 2021.

Noël, B., Van Kampenhout, L., Van De Berg, W. J., Lenaerts, J., Wouters, B., and Van Den Broeke, M. R.: Brief communication: CESM2 climate forcing (1950–2014) yields realistic Greenland ice sheet surface mass balance, The Cryosphere, 14, 1425–1435, 2020.

Noël, B., van Kampenhout, L., Lenaerts, J., van de Berg, W., and Van Den Broeke, M.: A 21st century warming threshold for sustained Greenland ice sheet mass loss, Geophysical Research Letters, 48, e2020GL090 471, 2021.

Noël, B., Lenaerts, J. T., Lipscomb, W. H., Thayer-Calder, K., and van den Broeke, M. R.: Peak refreezing in the Greenland firn layer under future warming scenarios, Nature Communications, 13, 6870, 2022.

Payne, A. J., Nowicki, S., Abe-Ouchi, A., Agosta, C., Alexander, P., Albrecht, T., Asay-Davis, X., Aschwanden, A., Barthel, A., Bracegirdle, T. J., et al.: Future sea level change under coupled model intercomparison project phase 5 and phase 6 scenarios from the Greenland and Antarctic ice sheets, Geophysical Research Letters, 48, e2020GL091 741, 2021.

https://doi.org/10.5194/tc-2023-154
Preprint. Discussion started: 10 October 2023

Plach, A., Nisancioglu, K. H., Langebroek, P. M., Born, A., and Le Clec'H, S.: Eemian Greenland ice sheet simulated with a higher-order model shows strong sensitivity to surface mass balance forcing, The Cryosphere, 13, 2133–2148, 2019.

Robinson, A., Calov, R., and Ganopolski, A.: Multistability and critical thresholds of the Greenland ice sheet, Nature Climate Change, 2, 429–432, 2012.

Robinson, A., Goldberg, D., and Lipscomb, W. H.: A comparison of the stability and performance of depth-integrated ice-dynamics solvers, The Cryosphere, 16, 689–709, 2022.

Rutt, I. C., Hagdorn, M., Hulton, N., and Payne, A.: The Glimmer community ice sheet model, Journal of Geophysical Research: Earth Surface, 114, 2009.

Sellevold, R. and Vizcaíno, M.: Global warming threshold and mechanisms for accelerated Greenland ice sheet surface mass loss, Journal of Advances in Modeling Earth Systems, 12, e2019MS002 029, 2020.

Sommers, A. N., Otto-Bliesner, B. L., Lipscomb, W. H., Lofverstrom, M., Shafer, S. L., Bartlein, P. J., Brady, E. C., Kluzek, E., Leguy, G., Thayer-Calder, K., et al.: Retreat and Regrowth of the Greenland Ice Sheet During the Last Interglacial as Simulated by the CESM2-CISM2 Coupled Climate–Ice Sheet Model, Paleoceanography and Paleoclimatology, 36, e2021PA004 272, 2021.

The IMBIE Team: Mass balance of the Greenland Ice Sheet from 1992 to 2018, Nature, 579, 233–239, 2020.

Van Breedam, J., Goelzer, H., and Huybrechts, P.: Semi-equilibrated global sea-level change projections for the next 10 000 years, Earth System Dynamics Discussions, 2020, 1–35, 2020.

van Kampenhout, L., Lenaerts, J. T., Lipscomb, W. H., Lhermitte, S., Noël, B., Vizcaíno, M., Sacks, W. J., and van den Broeke, M. R.: Present-day Greenland ice sheet climate and surface mass balance in CESM2, Journal of Geophysical Research: Earth Surface, 125, e2019JF005 318, 2020.

Vizcaino, M., Mikolajewicz, U., Ziemen, F., Rodehacke, C. B., Greve, R., and van den Broeke, M. R.: Coupled simulations of Greenland Ice Sheet and climate change up to AD 2300, Geophysical Research Letters, 42, 3927–3935, 2015.

Zeitz, M., Reese, R., Beckmann, J., Krebs-Kanzow, U., and Winkelmann, R.: Impact of the melt–albedo feedback on the future evolution of the Greenland Ice Sheet with PISM-dEBM-simple, The Cryosphere, 15, 5739–5764, 2021.

Zeitz, M., Haacker, J. M., Donges, J. F., Albrecht, T., and Winkelmann, R.: Dynamic regimes of the Greenland Ice Sheet emerging from interacting melt–elevation and glacial isostatic adjustment feedbacks, Earth System Dynamics, 13, 1077–1096, 2022.

https://doi.org/10.5194/tc-2023-154
Preprint. Discussion started: 10 October 2023

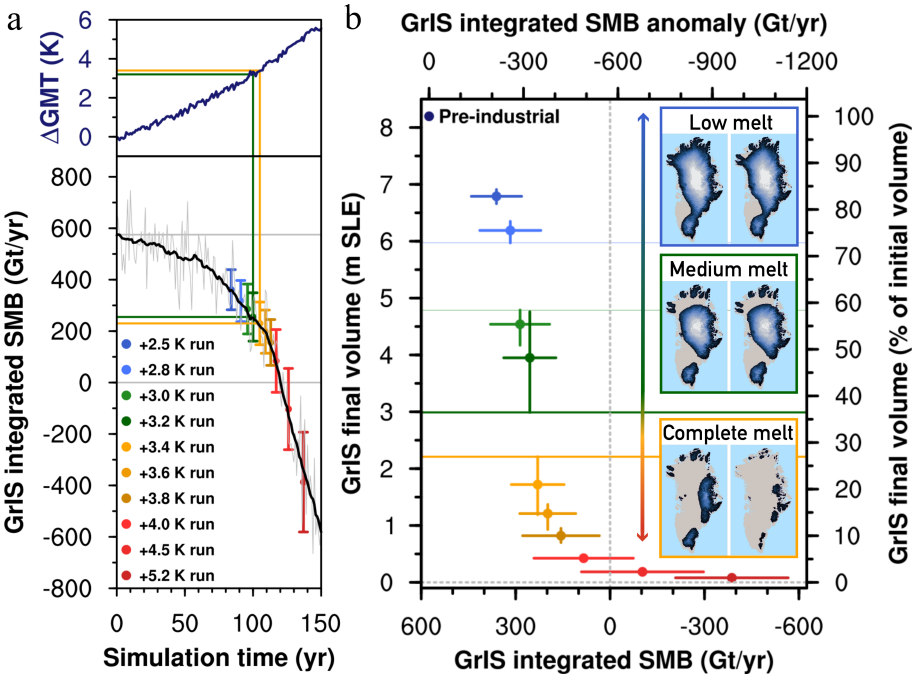

Figure 1. **(a)** Timeseries of (upper panel) Global Mean Temperature (GMT) anomaly relative to pre-industrial and (bottom panel) GrIS integrated Surface Mass Balance in the fully coupled BG-1pct simulation (Muntjewerf et al., 2020b). In the bottom panel, the SMB forcing used in our simulations (avg±stddev) is indicated in different colors for each run (see the inset legend). Green and yellow lines highlight the transition between "medium" to "complete" GrIS melt. **(b)** Scatter plot of GrIS integrated SMB forcing (avg±stddev, x-axis) *vs* GrIS final volume (avg±min/max, y-axis) in each simulation. Colors for each simulation as in the inset legend in (a). In the inset maps, GrIS final extent is showed for two simulations belonging in each group (for the "complete melt" group, +3.2 K and +4.0 K runs are shown).

https://doi.org/10.5194/tc-2023-154
Preprint. Discussion started: 10 October 2023

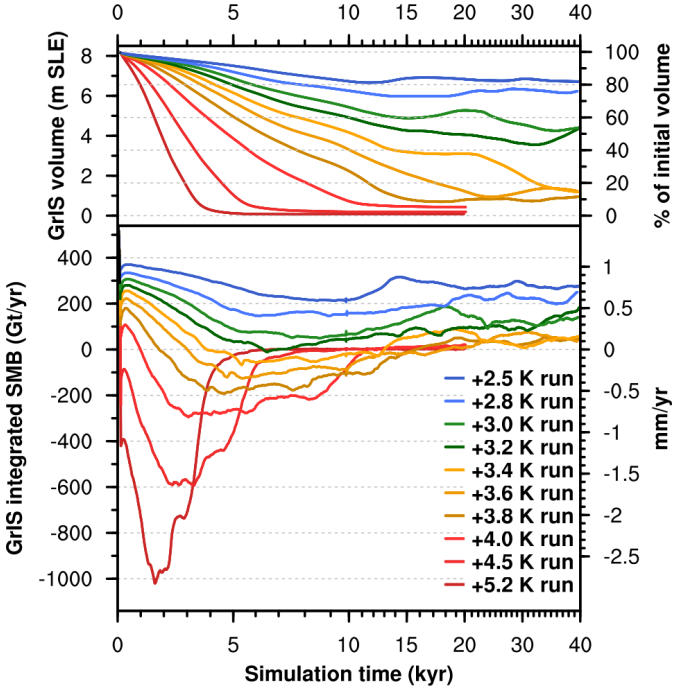

Figure 2. Timeseries of (upper panel) GrIS volume and (bottom panel) integrated Surface Mass Balance for the main runs presented in this study. Note that simulation time in the x-axis is irregular (minor tickmarks every 1000 years).

https://doi.org/10.5194/tc-2023-154
Preprint. Discussion started: 10 October 2023

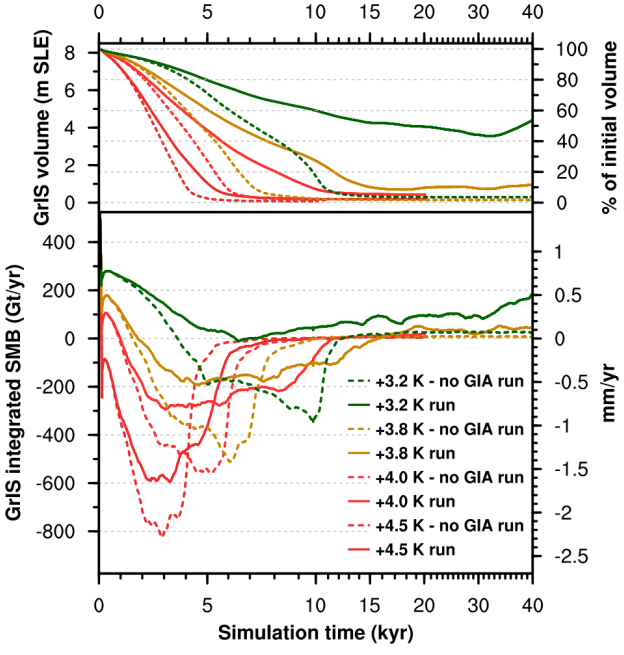

Figure 3. Timeseries of (upper panel) GrIS volume and (bottom panel) integrated Surface Mass Balance for selected sensitivity simulations with GIA turned on (solid lines) and GIA turned off (dashed lines). Note that simulation time in the x-axis is irregular (minor tickmarks every 1000 years).

https://doi.org/10.5194/tc-2023-154
Preprint. Discussion started: 10 October 2023

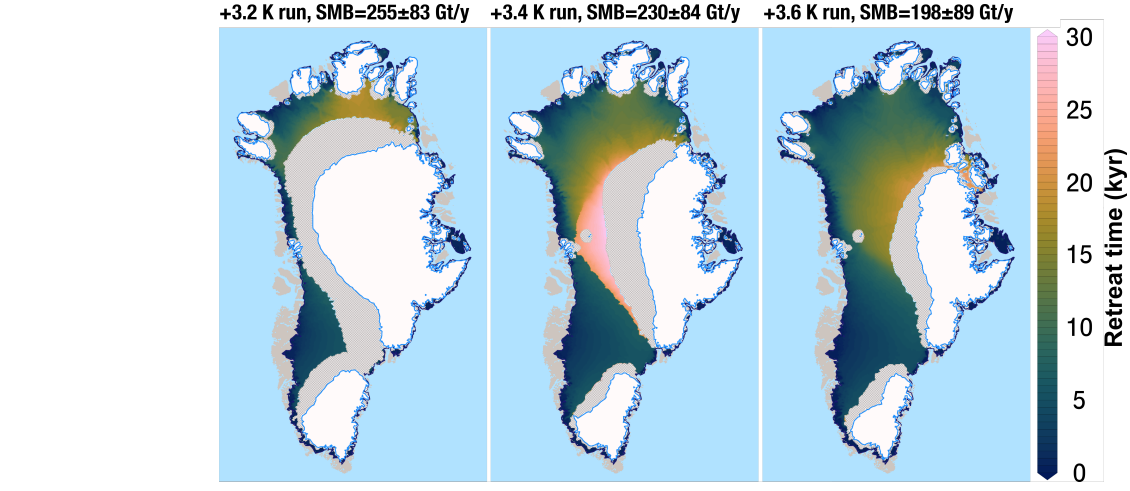

Figure 4. Map of GrIS retreat time for the (left) +3.2 K run, (center) +3.4 K run, (right) +3.6 K run. Ice-sheet areas showing GIA-induced margin oscillations are shown in grey, whereas areas continuously ice-covered throughout each run are filled in white.

https://doi.org/10.5194/tc-2023-154
Preprint. Discussion started: 10 October 2023

The Cryosphere Discussions
Open Access
EGU

ΔGMT	ΔGrISMT	SMB (avg ± stddv)	ΔSMB	Final vol. (min/**avg**/max)	Min. vol. time
Low melt					
+2.5 K	+2.0 K	361±80 Gt/yr	-230 Gt/yr	6.66 / **6.79** / 6.91 m SLE	11 kyrs
+2.8 K	+2.2 K	317±97 Gt/yr	-274 Gt/yr	5.97 / **6.19** / 6.35 m SLE	14 kyrs
Medium melt					
+3.0 K	+2.7 K	286±94 Gt/yr	-305 Gt/yr	4.17 / **4.54** / 4.79 m SLE	35 kyrs
+3.2 K	+2.9 K	255±83 Gt/yr	-336 Gt/yr	2.99 / **3.95** / 4.76 m SLE	31 kyrs
Complete melt					
+3.4 K	+3.2 K	230±84 Gt/yr	-361 Gt/yr	1.19 / **1.72** / 2.21 m SLE	40 kyrs
+3.6 K	+3.7 K	198±89 Gt/yr	-392 Gt/yr	0.93 / **1.21** / 1.37 m SLE	25 kyrs
+3.8 K	+4.0 K	156±122 Gt/yr	-435 Gt/yr	0.70 / **0.82** / 0.95 m SLE	17 kyrs
+4.0 K	+4.2 K	84±158 Gt/yr	-507 Gt/yr	0.43 / **0.42** / 0.42 m SLE	12 kyrs
+4.5 K	+5.0 K	-103±194 Gt/yr	-695 Gt/yr	0.18 / **0.19** / 0.19 m SLE	8 kyrs
+5.2 K	+5.9 K	-387±179 Gt/yr	-978 Gt/yr	0.07 / **0.08** / 0.09 m SLE	5 kyrs

Table 1. First four columns: values from each of the 23 years-long intervals in the fully coupled BG-1pct run used to force our simulations (transient global mean and GrIS anomaly to pre-industrial, GrIS integrated SMB, GrIS integrated SMB anomaly to pre-industrial). In the last two columns, final GrIS volume (minimum/average/maximum) and time needed to reach minimum GrIS volume in our simulations.

https://doi.org/10.5194/tc-2023-154
Preprint. Discussion started: 10 October 2023

Runs	Pre-ind.	Contemporary (1995-2014)	Mid-century (2031-2050)	End-of-century (2080-2099)
CESM2/CISM2				
Pre-ind.	591±83 Gt/yr			
Hist.		571±80 Gt/yr		
SSP5-8.5			359±84 Gt/yr	-511±283 Gt/yr
CESM2-only				
Hist.		390±28 Gt/yr		
SSP1-2.6			252±65 Gt/yr	88±97 Gt/yr
SSP2-4.5			267±58 Gt/yr	21±80 Gt/yr
SSP3-7.0			227±76 Gt/yr	-269±106 Gt/yr
SSP5-8.5			192±90 Gt/yr	-906±307 Gt/yr

Table 2. Comparison of GrIS integrated Surface Mass Balance (avg±stddev) for fully coupled CESM2/CISM2 simulations and CESM2-only simulations for pre-industrial, historical and available SSP scenarios contributing to CMIP6. Note that in the CESM2-only runs the Surface Mass Balance is calculated and integrated over the prescribed, present-day observed GrIS elevation.

https://doi.org/10.5194/tc-2023-154
Preprint. Discussion started: 10 October 2023

The Cryosphere
Discussions
Open Access
EGU

Appendix A: Supplementary Figures and Tables

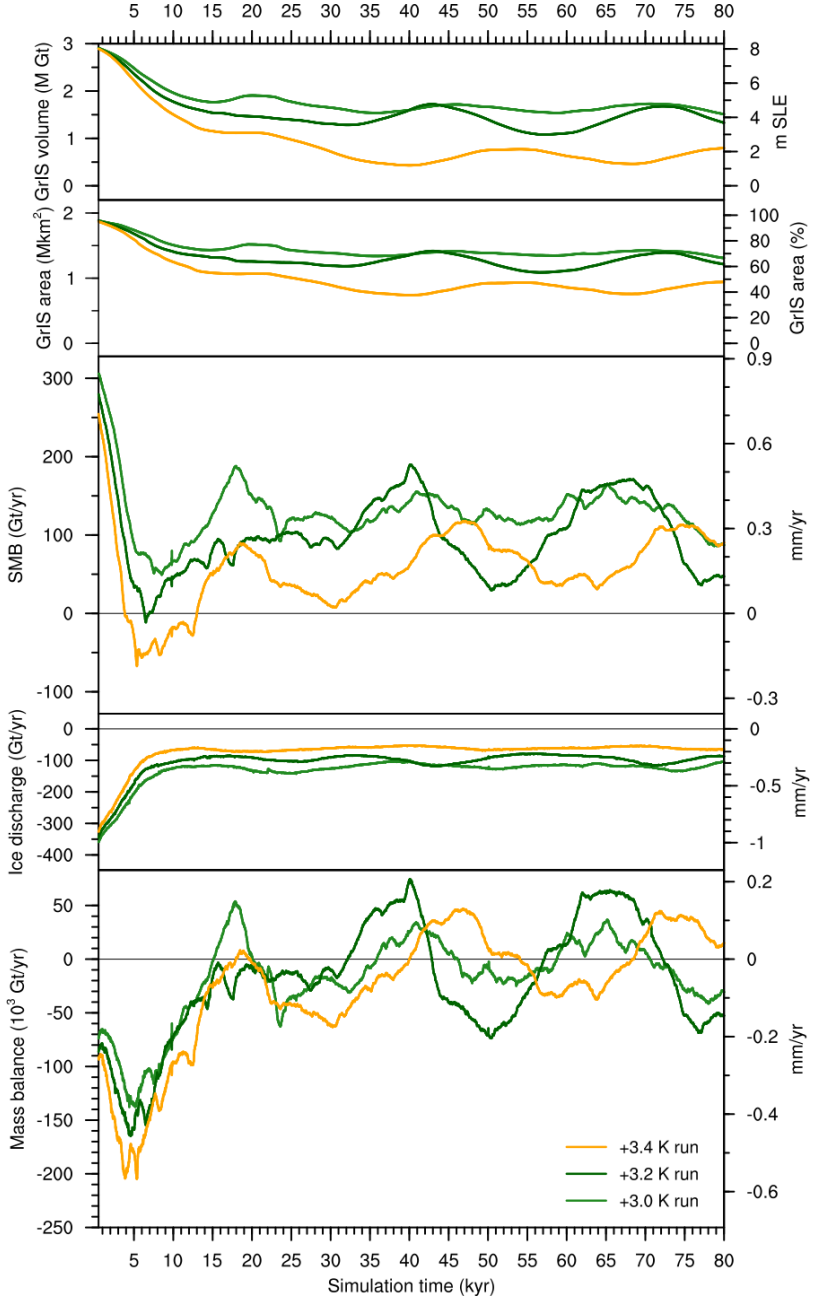

Figure A1. Timeseries of GrIS volume, area, Surface Mass Balance, ice discharge and mass balance for selected simulations extended until 80 kyrs, to show the quasi-periodicity of GIA-induced oscillations.

https://doi.org/10.5194/tc-2023-154
Preprint. Discussion started: 10 October 2023

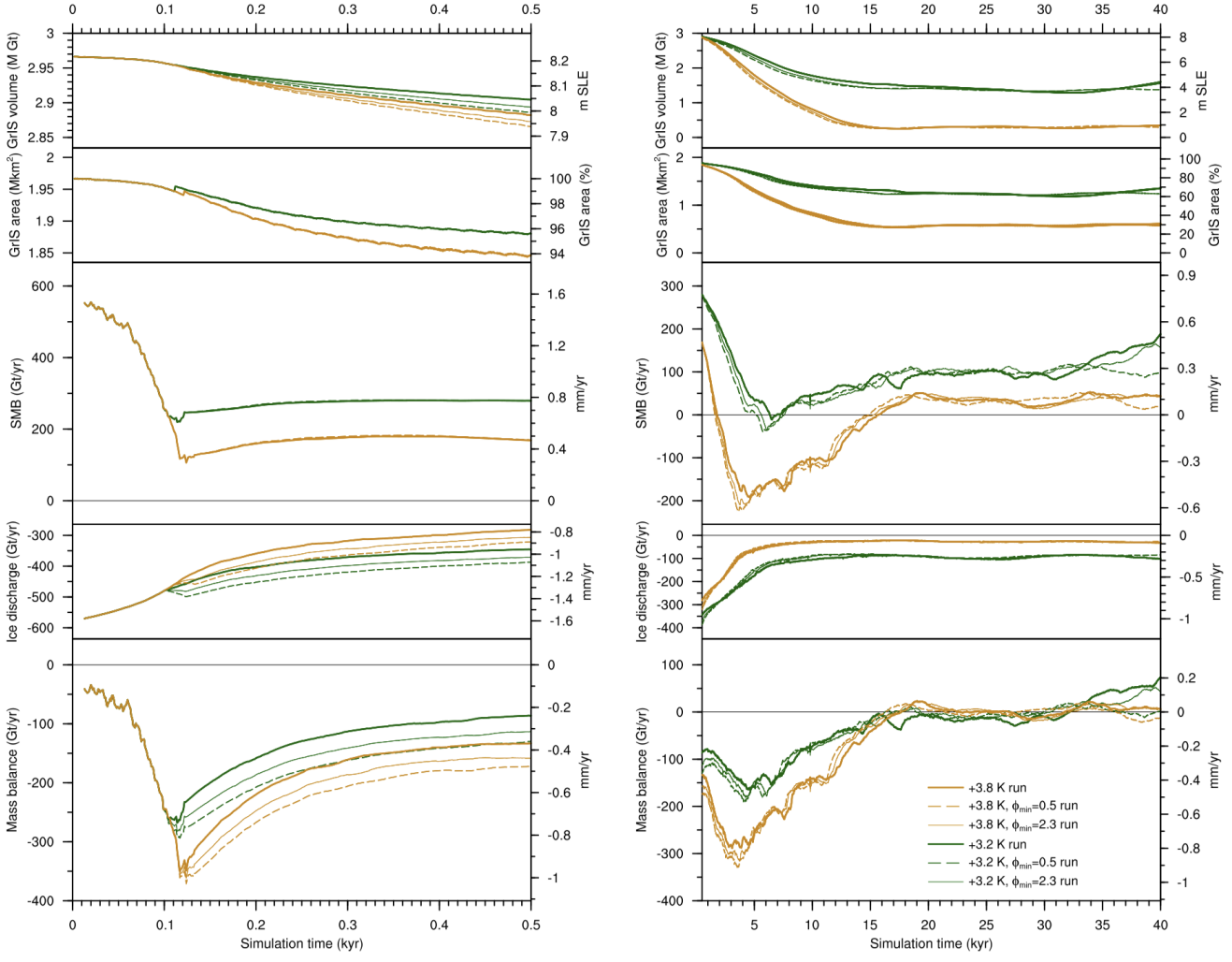

Figure A2. Timeseries of GrIS volume, area, Surface Mass Balance, ice discharge and mass balance for selected sensitivity simulations with increased ice discharge through reduced minimum friction angle in pseudo-plastic sliding law (solid thick line: ϕ_{min}=5, solid thin line: ϕ_{min}=2.3, dashed line: ϕ_{min}=0.5. On the left, values between in the first 500 years are shown. On the right, we show values between 500 and 40,000 years.

https://doi.org/10.5194/tc-2023-154
Preprint. Discussion started: 10 October 2023

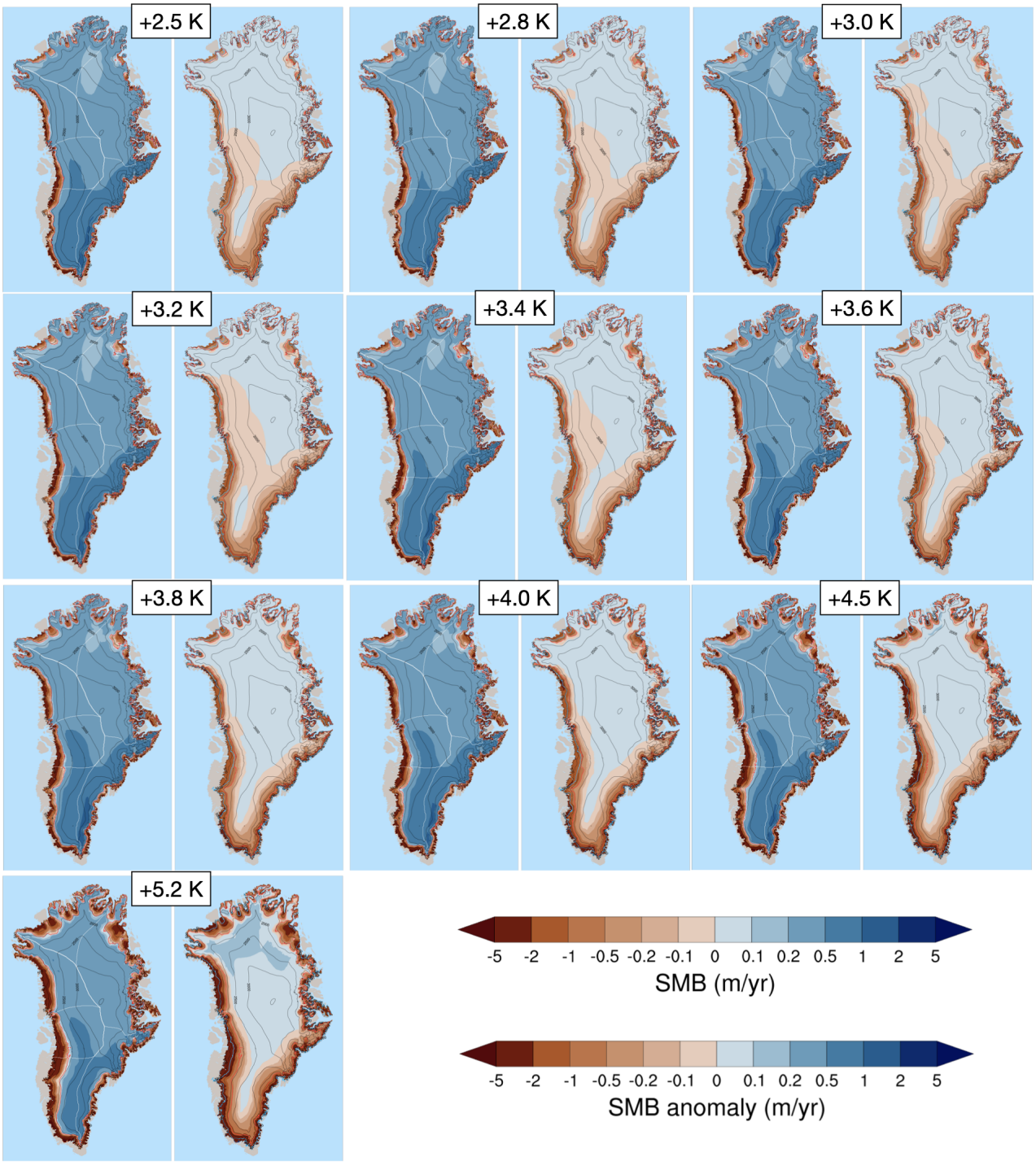

Figure A3. Average SMB forcing for each simulation (left: absolute values, right: anomaly to pre-industrial SMB simulated with CESM2/CISM2, Lofverstrom et al. (2020)).

https://doi.org/10.5194/tc-2023-154
Preprint. Discussion started: 10 October 2023

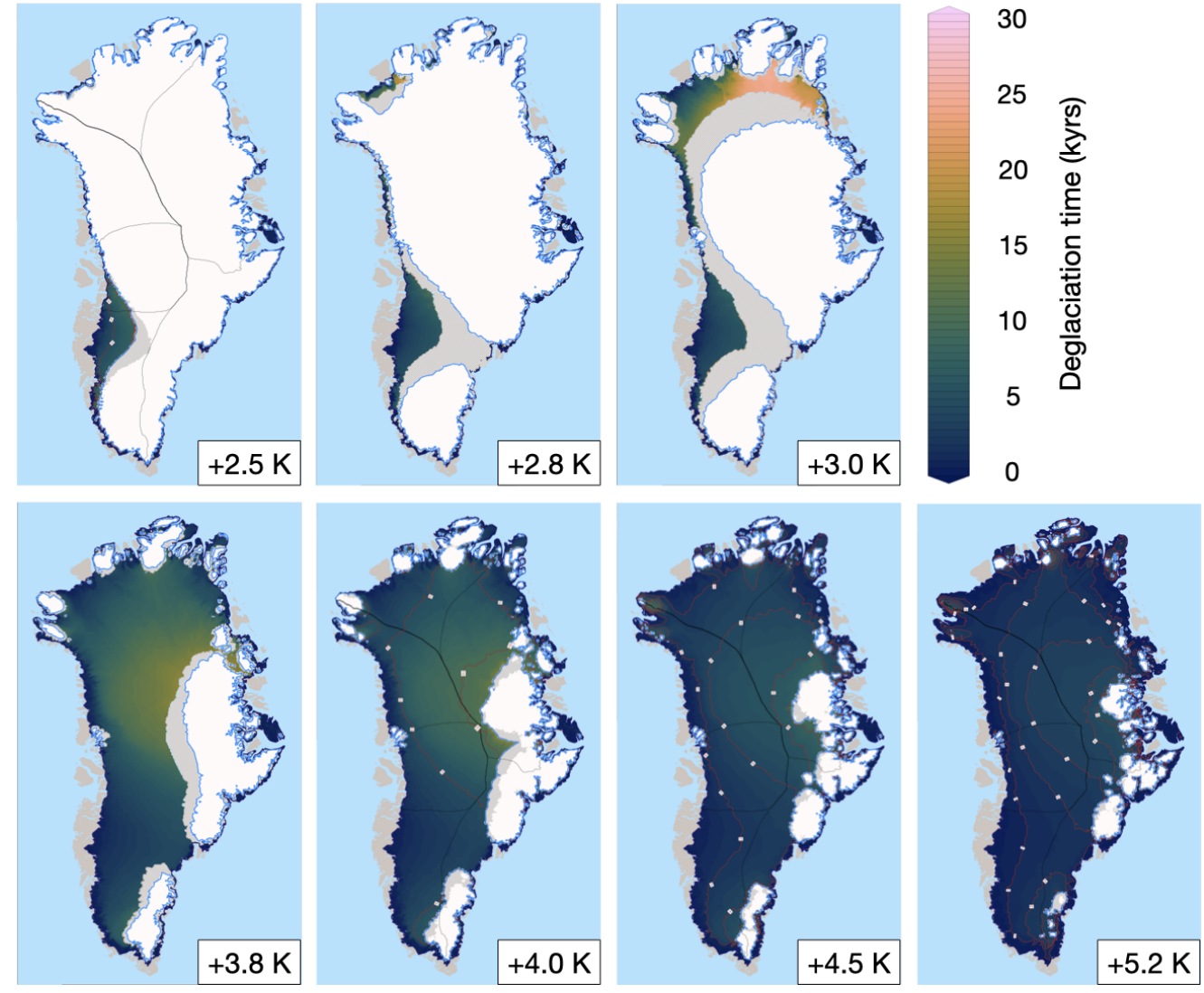

Figure A4. Map of GrIS retreat time for the simulations not shown in Fig. 4. Ice-sheet areas showing GIA-induced margin oscillations are shown in grey, whereas areas continuously ice-covered throughout each run are filled in white.

https://doi.org/10.5194/tc-2023-154
Preprint. Discussion started: 10 October 2023

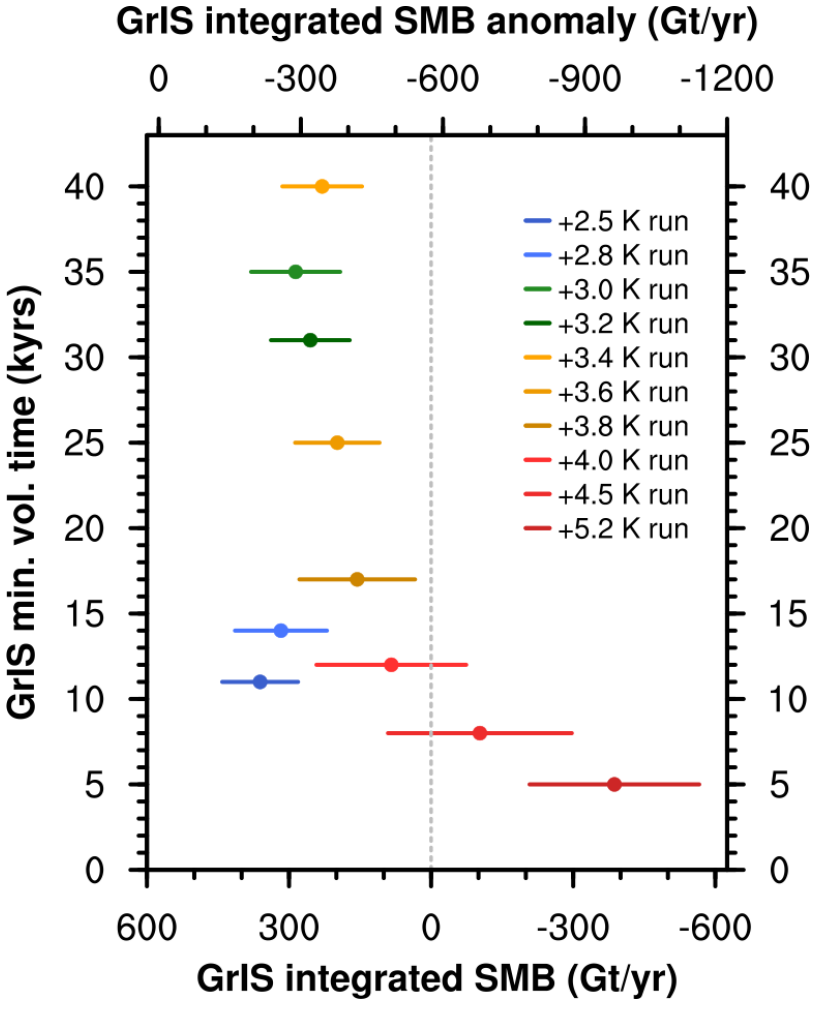

Figure A5. Scatter plot of GrIS integrated SMB forcing (avg±stddev, x-axis) *vs* time needed to reach minimum GrIS volume in our simulations (y-axis) in each simulation.

https://doi.org/10.5194/tc-2023-154
Preprint. Discussion started: 10 October 2023

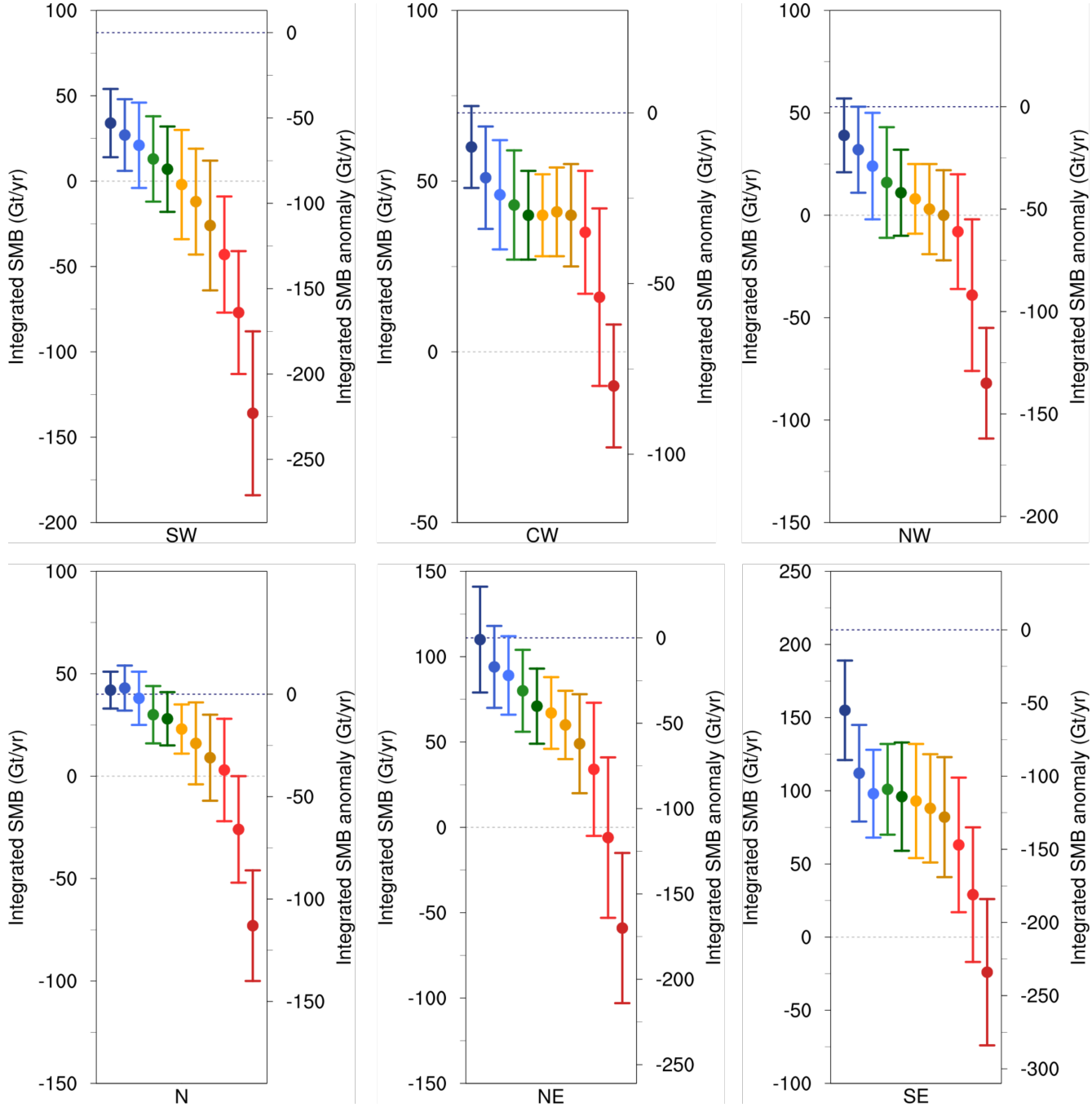

Figure A6. Forcing Surface Mass Balance (avg±stddev) in each run integrated over each IMBIE basin, following the basin definition as in "Rignot, E., & Mouginot, J. (2012). Ice flow in Greenland for the international polar year 2008–2009. Geophysical Research Letters, 39(11)."

https://doi.org/10.5194/tc-2023-154
Preprint. Discussion started: 10 October 2023


The Cryosphere Discussions
Open Access
EGU

Parameter	Short description	Value
F_g	Constant geothermal heat flux	0.05 W/m^2
$\phi_{\max}$	Maximum friction angle in pseudo-plastic sliding law, for B $\geq$ B$_{\max}$	40°
$\phi_{\min}$	Minimum friction angle in pseudo-plastic sliding law, for B $\leq$ B$_{\max}$	5°
B$_{\max}$	Bed elevation above which $\phi = \phi_{\max}$	700 m
B$_{\min}$	Bed elevation below which $\phi = \phi_{\min}$	-300 m
q	Exponent for pseudo-plastic sliding law	0.5
u0	Threshold velocity for pseudo-plastic sliding law	100 m/yr
$l_{\rm p}$	Lithosphere update period	100 yr
τ_r	Characteristic mantle relaxation time	3000 yr

Table A1. Model parameters used in the main CISM2 simulations presented in this study (note that in sensitivity tests with increased sliding we used a lower value for the minimum friction angle in pseudo-plastic sliding law.)

https://doi.org/10.5194/tc-2023-154
Preprint. Discussion started: 10 October 2023

Simulations	Forcing years	SMB (avg $\pm$ stddv)	ΔSMB
+2.5 K	74-96	361 $\pm$ 80 Gt/yr	-274 Gt/yr
+2.8 K	81-103	317 $\pm$ 97 Gt/yr	-305 Gt/yr
+3.0 K	86-108	286 $\pm$ 94 Gt/yr	-336 Gt/yr
+3.2 K	90-112	255 $\pm$ 83 Gt/yr	-361 Gt/yr
+3.4 K	95-117	230 $\pm$ 84 Gt/yr	-392 Gt/yr
+3.6 K	99-101	198 $\pm$ 89 Gt/yr	-435 Gt/yr
+3.8 K	103-125	156 $\pm$ 122 Gt/yr	-435 Gt/yr
+4.0 K	107-129	84 $\pm$ 158 Gt/yr	-507 Gt/yr
+4.5 K	116-138	-103 $\pm$ 194 Gt/yr	-695 Gt/yr
+5.2 K	131-150	-387 $\pm$ 179 Gt/yr	-978 Gt/yr

Table A2. Values from each of the 23 years-long intervals in the fully coupled BG-1pct run used to force our simulations (transient global mean anomaly to pre-industrial, initial and final forcing years, GrIS integrated SMB, GrIS integrated SMB anomaly to pre-industrial).